

Ultra Slow EM Wave Propagation Characteristics of Left-Handed Material Loaded Helical Guide

Dushyant K. Sharma* and Surya K. Pathak

Abstract—The dispersion characteristics (ω - β diagram) of a left-handed material (LHM) loaded helical guide is analytically solved and numerically computed for different medium properties as well as helical guide parameters. The modal behaviour of this structure has been studied with an aim to achieve ultra slow EM wave over wide bandwidth which finds potential applications in optical switches and memories for optical processing. Significant amount of phase velocity reduction has been achieved in comparison to when helix is in free space or loaded with normal dielectric medium. Other modal properties such as presence of two fundamental modes — backward and forward wave and their lower cut-off frequency (LCF) as well as the bandwidth spectrum is also revealed thoroughly.

1. INTRODUCTION

Left-handed material (LHM) is a novel material having negative permittivity ϵ and permeability μ value which is usually uncommon in any practical or engineering material applications. In 1964, Veselago [1] first studied the electrodynamics of such materials and described that phase velocity is anti-parallel to group velocity which exhibits backward wave properties of such materials. Due to that it also called backward wave material or LHM. In 2001, Smith et al. [2] experimentally verified the existence of LHM by designing metamaterial by thin wire (for negative permittivity) and split ring resonator (for negative permeability) [3]. The spectra of resonance where material behave like metamaterial can be changed by varying the physical size of the cell (containing split ring resonators and thin wires).

Enormous research interest has been shown by different research groups [4–8, 14–16] around the world to exploit this property for different engineering as well as physical sciences applications [17–21]. One such application is to find out the electromagnetic complex mode behaviour and wave steering properties (also called dispersion engineering) of different electromagnetic structures. When these structures are either embedded with metamaterial or the structure itself made up of metamaterial. Cory and Blum [4] studied surface wave propagation along metamaterial cylindrical guide for both real and imaginary transverse wave-number and found that transverse propagation coefficient of first TE_z and TM_z mode could be real or imaginary. Shu and Song [5] studied surface wave propagation in the grounded metamaterial slab in which they discussed about complex wave and evanescent surface wave mode. They observed that the value of normalized effective dielectric constant (ϵ_{eff}) for evanescent surface wave mode is high as compared to $\epsilon_{ri}\mu_{ri}$ (inside) and $\epsilon_{ro}\mu_{ro}$ (outside). Cory and Barger [6] studied metamaterial slab guide and observed that it can be used as filter due to appearance of band-pass region. Wu et al. [7] studied the guided mode in metamaterial slab having real and imaginary transverse wave number. They found that cut-off exists for all modes in real transverse wave number and guided mode are also present in imaginary transverse wave number. Baccarelli et al. [8] studied metamaterial grounded slab and presents condition for suppression of proper surface wave (ordinary and evanescent surface wave) that made considered structure a good candidate for planar antenna substrate.

Received 1 January 2014, Accepted 7 February 2014, Scheduled 12 February 2014

* Corresponding author: Dushyant Kumar Sharma (antsharma2@gmail.com).

The authors are with the Institute for Plasma Research, Bhat, Gandhinagar 382 428, India.

Ruppin [9] studied surface polaritons modes of a semi-infinite left-handed medium and demonstrated how they can be observed using the attenuated total reflection (ATR) technique. Darmany et al. [10] studied the properties of surface EM wave at the interface of left-handed and conventional medium and they observed that both p - and s -surface wave modes are not coexisted in same frequency range. They also calculated surface modes Poynting vector, density of energy and velocity of energy transfer. Kats et al. [11] also studied the EM surface wave at the interface of left-handed medium and demonstrated that 2D interfaces separating 3D metamaterial can exhibit properties of 2D left-handed media for surface waves. They found, total energy flux and group velocity of these waves are anti-parallel to the phase velocity. Leskova et al. [12, 13] studied scattering of an EM wave from, and its transmission through, a slab of random surface of a left-handed medium. Engheta [14] presented an idea of phase compensator using metamaterial in thin sub wavelength cavity.

In recent studies variety of materials have been investigated that have spectral resonant behaviour for achieving slow wave [22, 23]. That effect could be produced in periodically arranged structures like artificial material (metamaterial or photonic crystal). Bait-Suwailam and Chen [15] studied metamaterial slab waveguide and found that both TM and TE modes travel slowly. Erfaninia and Rostami [24] also observed that group velocity is greatly reduced in passive multilayered metamaterial waveguide. In these studies it has been observed that presence of metamaterial medium slow down the wave velocity.

All above-mentioned studies are related to planar as well as cylindrical waveguides where complex mode behaviour has been studied in context of different applications. For a long-time Helical guide has been widely used in travelling wave tubes as a slow-wave structure. Recently, Baqir and Choudhury [25, 26] also proposed the use of helix in optical fibre to create the twisted clad and studied the energy flux propagation behaviour using DB boundary condition.

The motivation of present study is to superimpose the helical guide slow wave characteristics with LHM properties to achieve ultra slow EM wave over a wide bandwidth (BW). This paper is arranged as follows. In Section 2, the dispersion relation of LHM loaded helical guide derived. In Section 3, numerical/computational results have been analysed and presented. In Sections 4 and 5, results are discussed, summarized and concluded.

2. DISPERSION RELATION

The structure used for analysis is a sheath helix of radius a and pitch angle ψ as shown in Fig. 1. The diameter of the wires is infinitesimally small and infinite number of wires in a tape is assumed. Spacing between adjacent wires is very small at the same time they are insulated with each other. It conducts only in a direction making an angle ψ with plane tangential to the axis [27]. Region I is LHM media which is assumed to be non-dispersive, isotropic and homogeneous and region II is free space.

The Borgnis' potentials for LHM loaded helical guide of radius $\rho = a$ and for $e^{jn\phi}$ turn variations

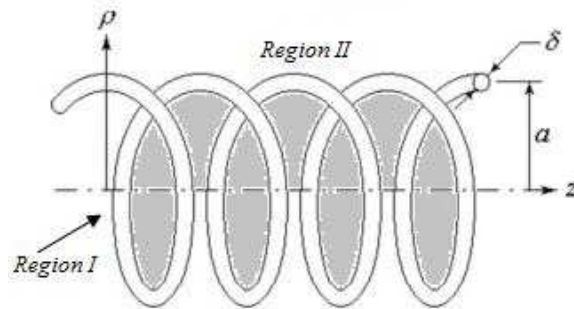


Figure 1. Helix of radius ‘ a ’, region I (inner region) is LHM media and region II (outer-region) is free-space.

are written as:

$$U_i = A_{n,i} C_{n,i}(k_i \rho) e^{jn\phi} e^{-j\beta z} \quad (1)$$

$$V_i = B_{n,i} C_{n,i}(k_i \rho) e^{jn\phi} e^{-j\beta z} \quad (2)$$

Here, $i = 1$ for region I ($\rho < a$) and $i = 2$ for region II ($\rho > a$). A_i and B_i are field coefficients, $C_{n,i}$ are needed Bessel functions of order n which describe modal behaviour of the wave.

The field equations in two regions are written as:

$$E_{z,i} = -k_i^2 A_i C_{n,i}(k_i \rho) e^{jn\phi} e^{-j\beta z} \quad (3)$$

$$E_{\rho,i} = \left[-j\beta k_i A_i C'_{n,i}(k_i \rho) + \frac{\omega \mu_i n}{\rho} B_i C_{n,i}(k_i \rho) \right] e^{jn\phi} e^{-j\beta z} \quad (4)$$

$$E_{\phi,i} = \left[\frac{n\beta}{\rho} A_i C_{n,i}(k_i \rho) + (j\omega \mu_i k_i) B_i C'_{n,i}(k_i \rho) \right] e^{jn\phi} e^{-j\beta z} \quad (5)$$

$$H_{z,i} = -k_i^2 B_i C_{n,i}(k_i \rho) e^{jn\phi} e^{-j\beta z} \quad (6)$$

$$H_{\rho,i} = \left[\frac{-\omega \epsilon_i n}{\rho} A_i C_{n,i}(k_i \rho) - j\beta k_i B_i C'_{n,i}(k_i \rho) \right] e^{jn\phi} e^{-j\beta z} \quad (7)$$

$$H_{\phi,i} = \left[-j\omega \epsilon_i k_i A_i C'_{n,i}(k_i \rho) + \frac{n\beta}{\rho} B_i C_{n,i}(k_i \rho) \right] e^{jn\phi} e^{-j\beta z} \quad (8)$$

Here, ($'$) is derivative of Bessel function with respect to its argument. ϵ_1 and μ_1 are media parameters of region I those are negative real numbers. ϵ_2 and μ_2 are positive real numbers. k_1 and k_2 are transverse wave numbers for region I and region II respectively, β is longitudinal phase coefficient. Relation between k_i and β is given by the equation:

$$k_i = \sqrt{\beta^2 - k_{oi}^2} \quad (9)$$

Here, $k_{oi} (= \omega \sqrt{\epsilon_i \mu_i})$ is propagation vector. For guided mode propagation, field in region II should decay exponentially in transverse direction. Due to that $C_{n,2}(k_2 \rho)$ is replaced by modified Bessel function of second kind $K_n(k_2 \rho)$. Due to skewed boundaries helical guide supports slow wave propagation therefore $C_{n,1}(k_1 \rho)$ is replaced by modified Bessel function of first kind $I_n(k_1 \rho)$.

At boundary ($\rho = a$), electric field is continuous in the direction of propagation and magnetic field is continuous normal to the direction of propagation. In term of ϕ and z , boundary conditions for helical guide at $\rho = a$, are written as [28]:

$$E_{z,1} = E_{z,2} \quad (10)$$

$$E_{\phi,1} = E_{\phi,2} \quad (11)$$

$$E_{z,1} = -E_{\phi,1} \cot(\psi) \quad (12)$$

$$E_{z,2} = -E_{\phi,2} \cot(\psi) \quad (13)$$

$$H_{z,1} + H_{\phi,1} \cot(\psi) = H_{z,2} + H_{\phi,2} \cot(\psi) \quad (14)$$

The field expressions from equation numbers (3)–(8) are substituted into the corresponding boundary conditions in Equations (10)–(14) and a set of four linear homogeneous equations with four unknown constants A_1 , A_2 , B_1 and B_2 are obtained. A non-trivial solution of the fields exists only if 4×4 determinants formed by the coefficients of the unknown constants in the set of equations vanish. The obtained determinant is:

$$\begin{vmatrix} m_1 & m_2 & 0 & 0 \\ 0 & 0 & m_3 & m_4 \\ m_5 & m_6 & m_7 & m_8 \\ m_9 & m_{10} & m_{11} & m_{12} \end{vmatrix}$$

where,

$$m_1 = \left(-k_1^2 \sin(\psi) + \frac{n\beta}{a} \cos(\psi) \right) I_n(k_1 a)$$

$$m_2 = j\omega \mu_1 k_1 \cos(\psi) I'_n(k_1 a)$$

$$\begin{aligned}
m_3 &= \left(-k_2^2 \sin(\psi) + \frac{n\beta}{a} \cos \psi \right) K_n(k_2a) \\
m_4 &= j\omega\mu_2 k_2 \cos(\psi) K'_n(k_2a) \\
m_5 &= \left(k_1^2 \cos(\psi) + \frac{n\beta}{a} \sin(\psi) \right) I_n(k_1a) \\
m_6 &= (j\omega\mu_1 k_1 \sin \psi) I'_n(k_1a) \\
m_7 &= - \left(k_2^2 \cos \psi + \frac{n\beta}{a} \sin \psi \right) K_n(k_2a) \\
m_8 &= -j\omega\mu_2 k_2 \sin(\psi) K'_n(k_2a) \\
m_9 &= j\omega\epsilon_1 k_1 \cos(\psi) I'_n(k_1a) \\
m_{10} &= \left(k_1^2 \sin(\psi) - \frac{n\beta}{a} \cos(\psi) \right) I_n(k_1a) \\
m_{11} &= -j\omega\epsilon_2 k_2 \cos(\psi) K'_n(k_2a) \\
m_{12} &= - \left(k_2^2 \sin(\psi) - \frac{n\beta}{a} \cos(\psi) \right) K_n(k_2a)
\end{aligned}$$

Equating determinant to zero results in eigen-value equation for β is:

$$\begin{aligned}
&k_o a^2 c \epsilon_1 k_1 \cot(\psi) \frac{I'_n(k_1a)}{I_n(k_1a)} - \frac{Y^2}{k_o a^2 c \mu_1 k_1 \cot(\psi)} \frac{I_n(k_1a)}{I'_n(k_1a)} \\
&- k_o a^2 c \epsilon_2 k_2 \cot(\psi) \frac{K'_n(k_2a)}{K_n(k_2a)} r^2 + \frac{X^2 r^2}{k_o a^2 c \mu_2 k_2 \cot(\psi)} \frac{K_n(k_2a)}{K'_n(k_2a)} = 0
\end{aligned} \tag{15}$$

Here $r = k_1a/k_2a$, $X = (k_2a)^2 - n\beta a \cot(\psi)$, $Y = (k_1a)^2 - n\beta a \cot(\psi)$, $k_o = \omega\sqrt{\epsilon_o\mu_o}$, ϵ_o and μ_o are free space permittivity and permeability.

The dispersion relation Equation (15) is further algebraically re-derived for various special cases:

1. For $n = 0$

$$\begin{aligned}
&k_o a^2 c \epsilon_1 k_1 \cot(\psi) \frac{I'_0(k_1a)}{I_0(k_1a)} - \frac{k_1a}{k_o a c \mu_1 \cot(\psi)} \frac{I_0(k_1a)}{I'_0(k_1a)} \\
&- k_o a^2 c \epsilon_2 k_2 \cot(\psi) \frac{K'_0(k_2a)}{K_0(k_2a)} r^2 + \frac{k_2 a r^2}{k_o a c \mu_2 \cot(\psi)} \frac{K_0(k_2a)}{K'_0(k_2a)} = 0
\end{aligned} \tag{16}$$

2. For $\psi = 0$ and $n = 0$

$$\frac{\epsilon_1 I'_n(k_1a)}{\epsilon_2 I_n(k_1a)} - r \frac{K'_n(k_2a)}{K_n(k_2a)} = 0 \tag{17}$$

3. For $\psi = 0$ and $n \neq 0$

$$k_o a c \left[\epsilon_1 k_1 a \frac{I'_n(k_1a)}{I_n(k_1a)} - r^2 \epsilon_2 k_2 a \frac{K'_n(k_2a)}{K_n(k_2a)} \right] - \frac{n^2 \beta^2}{k_o a c} \left[\frac{1}{\mu_1 k_1 a} \frac{I_n(k_1a)}{I'_n(k_1a)} - \frac{1}{\mu_2 k_2 a} \frac{K_n}{K'_n} \right] = 0 \tag{18}$$

4. For $\psi = 90$ and any n

$$r \frac{I'_n(k_1a)}{I_n(k_1a)} - \frac{\mu_1 K'_n(k_2a)}{\mu_2 K_n(k_2a)} = 0 \tag{19}$$

Propagation vectors in Equation (9) have been normalized with respect to helix radius a , in both the regions and are rewritten as:

For region-I:

$$k_1a = \sqrt{(\beta a)^2 - (k_{o1}a)^2} \tag{20}$$

For region-II:

$$k_2a = \sqrt{(\beta a)^2 - (k_{o2}a)^2} \tag{21}$$

By solving Equations (20) and (21) one can find:

$$k_2a = \sqrt{(k_1a)^2 + (k_{o1}a)^2 - (k_{o2}a)^2} \tag{22}$$

3. RESULTS AND ANALYSIS

Dispersion Equation (15) is a transcendental equation, which has been solved numerically as well as graphically to compute the longitudinal phase coefficient as a function of frequency k_0a . Mathematica 7.0 software package is used for finding out the roots numerically. Obtained roots are verified by graphical procedure. For that, βa in Equation (15) is replaced by $\sqrt{((k_{o1}ak_2a)^2 - (k_{o2}ak_1a)^2)/((k_1a)^2 - (k_2a)^2)}$ using Equations (20) and (21) and plotted between k_1a versus k_2a . Same variations are also plotted using Equation (22). Superposition of these two graphs (not shown here) provides the value of βa .

For surface wave propagation k_1a and k_2a should be positive. Due to that only those values of βa are considered as a root which are high as compared to $k_{o1}a$ and $k_{o2}a$.

3.1. Dominant Mode ($n = 0$)

In Fig. 2, normalized longitudinal phase coefficient ($k_0a/\beta a$) has been plotted as a function of propagation vector (k_0a) for three cases when helix is: (i) in free space, (ii) loaded with DPS material and (iii) loaded with LHM material. A comparative study has been made among three cases to understand complex mode propagation behaviour such as-backward wave mode, forward wave mode, phase velocity, and BW spectrum.

In case of LHM loading at low frequencies two fundamental modes (2 and 3 in Fig. 2) propagate simultaneously having LCF at $k_0a = 1.3$. Mode 3 having positive slope in dispersion graph and negative group velocity which exhibits a backward wave properties. At higher frequencies from $k_0a = 1.6$, onwards only forward ultra slow mode 2 propagates which has positive group velocity. As we increase the frequency normalize phase velocity ($k_0a/\beta a = v_p/c$) of mode 2 start to vary from 0.297 and it reduces to 0.040 at higher frequencies.

While in case of DPS medium mode 1 (in Fig. 2) have LCF at $k_0a = 0.3$. The normalized phase velocity varies from 0.690 and almost constant at 0.406 at higher frequencies ($k_0a = 7$) which is 1.23 times less as compared to free-space case (4 in Fig. 2).

Lowest achieved normalized phase velocity in LHM medium is 10 times less as compared to DPS medium. This implies that the presence of LHM medium enhances the slow wave behaviour of helical guide.

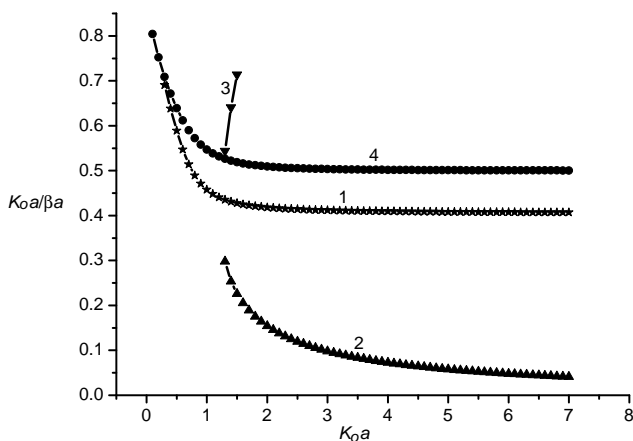


Figure 2. Variation of $k_0a/\beta a$ vs k_0a at $n = 0$ and $\psi = 30^\circ$. free-space case ($\epsilon_{r1} = 1, \mu_{r1} = 1$) represented by \circ , DPS material ($\epsilon_{r1} = 2, \mu_{r1} = 1$) loading represented by \star , LHM ($\epsilon_{r1} = -2, \mu_{r1} = -1$) loading represented by Δ and ∇ .

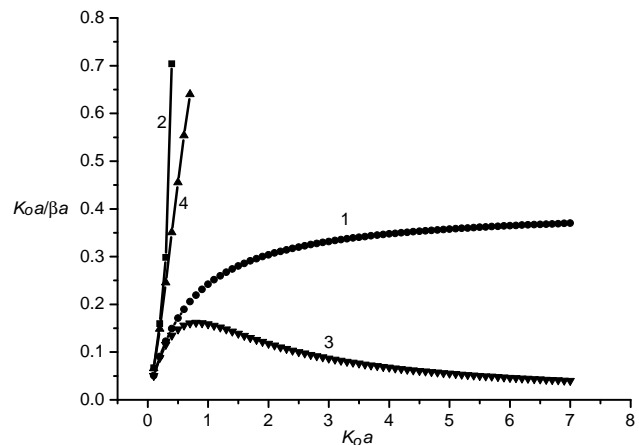


Figure 3. Variation of $k_0a/\beta a$ vs k_0a at $n = 1$ and $\psi = 30^\circ$. DPS material ($\epsilon_{r1} = 2, \mu_{r1} = 1$) loading represented by \circ and \square , LHM ($\epsilon_{r1} = -2, \mu_{r1} = -1$) loading represented by ∇ and Δ .

3.2. Higher Order Modes

Similar graphs are plotted for first ($n = 1$) higher order mode in Fig. 3. In case of LHM loading at low frequencies two fundamental modes (3 and 4 in Fig. 3) coexist in the guide. Mode 4 is a backward wave mode having positive slope in dispersion graph and negative group velocity. From $k_0a = 0.8$ onwards only forward ultra slow mode 3 exists in the guide. Normalized phase velocity of mode 3 starts to varies from 0.05 and increases up to $k_0a = 0.8$, afterwards it reduces and almost becomes constant at 0.04 for higher frequencies.

In case of DPS medium two fundamental modes, 1 (forward wave mode) and 2 (backward wave mode) are propagating (in Fig. 3) till $k_0a = 0.4$. After that only, forward wave mode propagates and its normalize phase velocity ($k_0a/\beta a = v_p/c$) vary from 0.05 to 0.36.

In case of LHM loading, slowest achieved normalized phase velocity is 0.04 which is 9 times lower as compared to their DPS medium counter-part. This again signifies the presence of LHM medium further increases the slow behaviour of helical guide.

3.3. Effect of Physical Design Parameter

Helical guide contains two design parameters namely radius (a) and pitch angle (ψ). In above results radius (a) is normalized with propagation vector k_0a , therefore its effect could be understood by making frequency constant. Helix pitch angle (ψ) effects on slow wave propagation behaviour have been shown in Figs. 4 and 5.

At lower frequencies two modes (backward and forward wave mode) propagate simultaneously. Modes described as 1, 3 and 5 (in Figs. 4 and 5) propagate as forward wave mode and modes 2, 4 and 6 (in Figs. 4 and 5) propagate as backward wave mode for pitch angles 30, 20, and 10 degrees respectively.

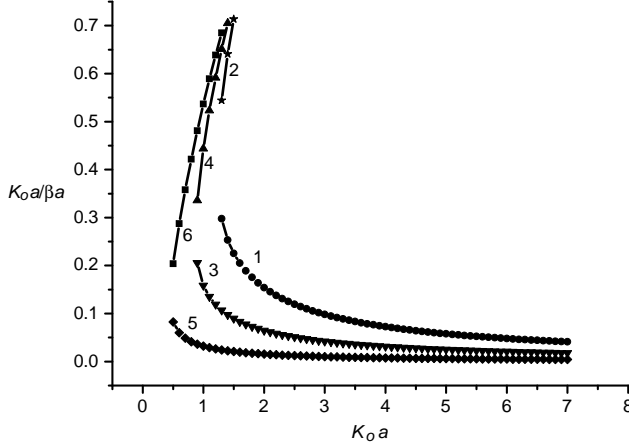


Figure 4. Variation of $k_0a/\beta a$ vs k_0a at $n = 0$ in LHM ($\epsilon_{r1} = -2$, $\mu_{r1} = -1$) loading for $\psi = 30^\circ$ represented by \star and \circ , 20° represented by ∇ and Δ and 10° represented by \diamond and \square .

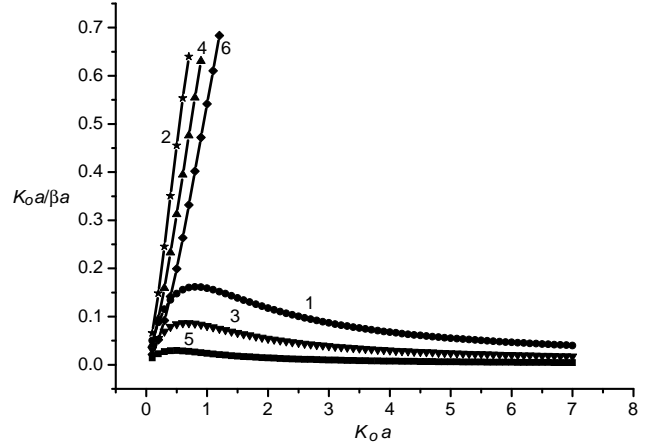


Figure 5. Variation of $k_0a/\beta a$ vs k_0a at $n = 1$ in LHM ($\epsilon_{r1} = -2$, $\mu_{r1} = -1$) loading for $\psi = 30^\circ$ represented by \star and \circ , 20° represented by ∇ and Δ and 10° represented by \diamond and \square .

Table 1. LCF of dominate mode ($n = 0$) and V_p/c of dominate and first higher order mode ($n = 1$) for different pitch angles.

ψ	LCF in k_0a	V_p/c ($n = 0$) at $k_0a = 7$	V_p/c ($n = 1$) at $k_0a = 7$
30°	1.3	0.0409	0.0400
20°	0.9	0.0177	0.0175
10°	0.5	0.0043	0.0043

In dominate mode, BW spectrum of backward wave mode increases with reduction in pitch angle (BW in 30° is $k_0a = 1.3$ to 1.5, 20° is $k_0a = 0.9$ to 1.4 and 10° is $k_0a = 0.5$ to 1.3). Similar observations are seen in higher order ($n = 1$) mode (BW in 30° is $k_0a = 0$ to 0.7, 20° is $k_0a = 0$ to 0.9 and 10° is $k_0a = 0$ to 1.2).

Normalized phase velocity of forward wave mode (1, 3 and 5 in Figs. 4 and 5) decreases as decrease in pitch angle (summarized in Table 1) that enhances the ultra slow wave behaviour of the helical guide.

3.4. Effect of LHM Medium on Guide Dispersion Behaviour

LHM media properties (ϵ_1 and μ_1) play very important role in reducing the phase velocity of the wave in order to achieve ultra slow wave. Three representative examples: (a) case I ($\epsilon_{r1} = -1.5, \mu_{r1} = -1; \epsilon_{r2} = 1, \mu_{r2} = 1$) (b) case II ($\epsilon_{r1} = -2, \mu_{r1} = -1; \epsilon_{r2} = 1, \mu_{r2} = 1$) and (c) case III ($\epsilon_{r1} = -5, \mu_{r1} = -1; \epsilon_{r2} = 1, \mu_{r2} = 1$) are considered for analysing these effects by varying ϵ_{r1} and keeping μ_{r1} constant.

In dominate mode, BW spectrum of backward wave mode (2 and 4 in Fig. 6) reduces (BW in case I is $k_0a = 2.1$ to 2.4 and in case II is $k_0a = 1.3$ to 1.5) with increase in $|\epsilon_{r1}|$ and it disappears in case III. Opposite to that BW spectrum of forward wave mode (1, 3 and 5 in Fig. 6) increase due to reduction in lower cut-off value (summarized in Table 2). Observed normalised phase velocity of forward wave mode is almost 8 times slower in case III as compared to case I reported in Table 2, which attributes the role of LHM properties in order to achieve ultra slow wave.

Similar observation is found in first higher order ($n = 1$) mode where BW spectra of backward wave mode (2, 4, and 5 in Fig. 7) reduces (BW in case I is $k_0a = 0$ to 1.4, case II is $k_0a = 0$ to 0.7 and

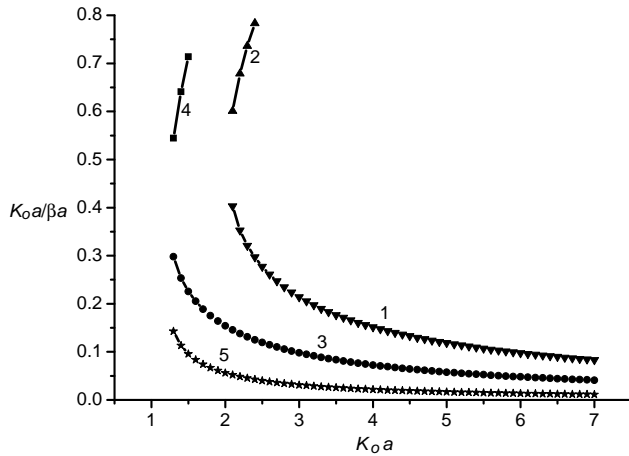


Figure 6. Variation of $k_0a/\beta a$ vs k_0a at $n = 0$ and $\psi = 30^\circ$, for case I ($\epsilon_{r1} = -1.5, \mu_{r1} = -1; \epsilon_{r2} = 1, \mu_{r2} = 1$) represented by ∇ and Δ , case II ($\epsilon_{r1} = -2, \mu_{r1} = -1; \epsilon_{r2} = 1, \mu_{r2} = 1$) represented by \circ and \square , and case III ($\epsilon_{r1} = -5, \mu_{r1} = -1; \epsilon_{r2} = 1, \mu_{r2} = 1$) represented by \star .

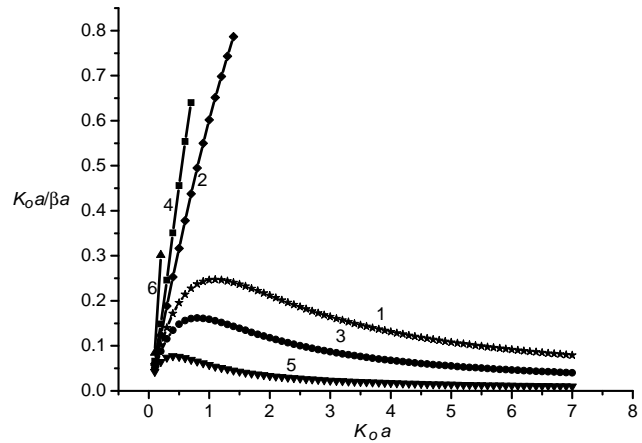


Figure 7. Variation of $k_0a/\beta a$ vs k_0a at $n = 1$ and $\psi = 30^\circ$, for case I ($\epsilon_{r1} = -1.5, \mu_{r1} = -1; \epsilon_{r2} = 1, \mu_{r2} = 1$) represented by \diamond and \star , case II ($\epsilon_{r1} = -2, \mu_{r1} = -1; \epsilon_{r2} = 1, \mu_{r2} = 1$) represented by \circ and \square , and case III ($\epsilon_{r1} = -5, \mu_{r1} = -1; \epsilon_{r2} = 1, \mu_{r2} = 1$) represented by ∇ and Δ .

Table 2. LCF of dominate mode ($n = 0$) and V_p/c of dominate and higher order mode ($n = 1$) in different cases.

Case	LCF ($n = 0$) in k_0a	V_p/c ($n = 0$) at $k_0a = 7$	V_p/c ($n = 1$) at $k_0a = 7$
case I	2.1	0.0830	0.0792
case II	1.3	0.0409	0.0400
case III	0.6	0.0101	0.0101

case III is $k_o a = 0$ to 0.2) with increase in $|\epsilon_{r1}|$. The normalized phase velocity of forward wave mode is summarized in Table 2.

4. DISCUSSION

In above analysis, it has been observed that due to higher value of longitudinal phase coefficient (β), phase velocity of wave is greatly reduced as compared to normal helical guide.

Modal behaviour study reveals that two fundamental modes, backward and forward wave modes, propagate simultaneously. BW of backward wave mode is very small and it dies off very fast. On the other hand forward wave mode has very high frequency spectrum. It has been found that normalized phase velocity, decreases with increase in $|\epsilon_{r1}|$. Similar variation is also observed when the guide pitch angle is reduced. For higher frequency spectrum, dispersion plot has similar behaviour but having a lower phase and group velocity.

The minimum phase velocity is observed in case III with pitch angle $\psi = 10^\circ$. If guide radius is $a = 1$ mm and $k_o a = 50$ ($freq = 2.38$ THz) then wave propagates with speed of 45860.46 meter per second which is 6541 times less as compared to speed of light (in Fig. 8). This reduction can be further enhanced by optimizing the LHM properties as well as helix dimensions.

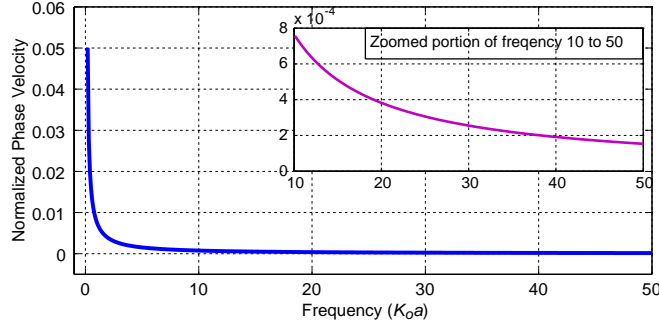


Figure 8. Variation of normalized phase velocity ($k_o a / \beta a$) vs frequency ($k_o a$) over a very large frequency range (up to THz) for the case III ($\epsilon_{r1} = -5$, $\mu_{r1} = -1$; $\epsilon_{r2} = 1$, $\mu_{r2} = 1$) at $n = 0$ and $\psi = 10^\circ$.

5. CONCLUSION

In this paper we introduce an idea of achieving ultra slow wave over wide BW by utilizing helical guide slow wave behaviour with LHM properties. This type of structure finds major application where controlled or tunable delay is required, such as optical switches, optical memories and microwave photonics. Another proposed future application of slow wave is in quantum computing.

REFERENCES

1. Veselago, V. G., "The electrodynamics of substances with simultaneous negative values of ϵ and μ ," *Soviet Phys. Uspekhi*, Vol. 1, No. 4, 509–514, 1968.
2. Shelby, R. A., D. R. Smith, and S. Schultz, "Experimental verification of a negative index of refraction," *Science*, Vol. 292, No. 5514, 77–79, 2001.
3. Pendry, J. B., "Negative refraction," *Contemporary Physics*, Vol. 45, No. 3, 191–202, 2004.
4. Cory, T. and T. Blum, "Surface-wave propagation along a metamaterial cylindrical guide," *Microwave and Optical Technology Letters*, Vol. 44, No. 1, 31–35, 2005.
5. Shu, W. and J. M. Song, "Complete mode spectrum of a grounded dielectric slab with double negative metamaterials," *Progress In Electromagnetics Research*, Vol. 65, 103–123, 2006.

6. Cory, T. and T. Barger, "Surface-wave propagation along a metamaterial slab," *Microwave and Optical Technology Letters*, Vol. 38, No. 5, 392–395, 2003.
7. Wu, B. I., T. M. Grzegorzczak, Y. Zhang, and J. A. Kong, "Guided modes with imaginary transverse wave number in a slab waveguide with negative permittivity and permeability," *Journal of Applied Physics*, Vol. 93, No. 11, 9386–9388, 2003.
8. Baccarelli, P., P. Burghignoli, F. Frezza, A. Galli, P. Lampariello, G. Lovat, and S. Paulotto, "Fundamental modal properties of surface waves on metamaterial grounded slabs," *IEEE Transactions on Microwave Theory and Techniques*, Vol. 53, No. 4, 1431–1442, 2005.
9. Ruppin, R., "Surface polaritons of a left-handed medium," *Physics Letters A*, Vol. 277, No. 1, 61–64, 2000.
10. Darmanyan, S. A., M. Neviere, and A. A. Zakhidov, "Surface modes at the interface of conventional and left-handed media," *Opt. Commun.*, Vol. 225, Nos. 4–6, 233–240, 2003.
11. Kats, A. V., S. Savelev, V. A. Yampolskii, and F. Nori, "Left-handed interfaces for electromagnetic surface waves," *Physical Review Letters*, Vol. 98, No. 7, 073901-1–073901-4, 2007.
12. Leskova, T. A., A. A. Maradudin, and I. Simonsen, "Scattering of electromagnetic waves from the random surface of a left-handed medium," *Proc. SPIE*, Vol. 4447, 6–16, 2001.
13. Leskova, T. A., A. A. Maradudin, and I. Simonsen, "Coherent scattering of an electromagnetic wave from, and its transmission through, a slab of a left-handed medium with a randomly rough illuminated surface," *Proc. SPIE*, Vol. 5189, 22–35, 2003.
14. Engheta, N., "An idea for thin subwavelength cavity resonators using metamaterials with negative permittivity and permeability," *IEEE Antennas and Wireless Propagation Letters*, Vol. 1, No. 1, 10–13, 2002.
15. Bait-Suwallam, M. M. and Z. Chen, "Surface-wave on a grounded double-negative (DNG) slab waveguide," *Microwave and Optical Technology Letters*, Vol. 44, No. 6, 494–498, 2003.
16. Shadrivov, I. V., A. A. Sukhorukov, and Y. S. Kivshar, "Guided modes in negative-refractive-index waveguides," *Physical Review E*, Vol. 67, 057602, 2003.
17. Shelby, R. A., D. R. Smith, S. C. Nemat-Nasser, and S. Schultz, "Microwave transmission through a two-dimensional, isotropic, left-handed metamaterial," *Applied Physics Letters*, Vol. 78, No. 4, 489–491, 2001.
18. Itoh, T., "Prospects for metamaterials," *Applied Physics Letters*, Vol. 40, No. 16, 972–973, 2004.
19. Itoh, T., "Cloaking a receiving antenna or a sensor with plasmonic metamaterials," *Metamaterials*, Vol. 4, Nos. 2–3, 153–159, 2010.
20. Gil, M., J. Bonache, and F. Martin, "Metamaterial filters: A review," *Metamaterials*, Vol. 2, No. 4, 186–197, 2008.
21. Pendry, J. B., "Negative refraction makes a perfect lens," *Physical Review Letters*, Vol. 85, No. 18, 3966–3969, 2000.
22. Hau, L. V., S. E. Harris, Z. Dutton, and C. H. Behroozi, "Light speed reduction to 17 metres per second in an ultracold atomic gas," *Letters of Nature*, Vol. 397, 594–598, 1999.
23. Bigelow, M. C., N. N. Lepeshkin, and R. W. Boyd, "Superluminal and slow light propagation in a room-temperature solid," *Science*, Vol. 301, No. 5630, 200–202, 2003.
24. Erfaninia, H. and A. Rostami, "Group velocity reduction in multilayer metamaterial waveguide," *Optik*, Vol. 124, No. 12, 1230–1233, 2013.
25. Baqir, M. A. and P. K. Choudhury, "Flux density through guides with microstructured twisted clad DB medium," *Journal of Nanomaterials*, Vol. 2014, 629651, 2014.
26. Baqir, M. A. and P. K. Choudhury, "Effects on the energy flux density due to pitch in twisted clad optical fibers," *Progress In Electromagnetics Research*, Vol. 139, 643–654, 2013.
27. Basu, B. N., *Electromagnetic Theory and Application in Beam-wave Electronics*, World Scientific, Singapore, 1996.
28. Zhang, K. and D. Li, *Electromagnetic Theory for Microwaves and Optoelectronic*, Springer, New York, 2008.